Formation of clusters in the ground state of the *t*–*J* model on a two-leg ladder

2004 J. Phys.: Condens. Matter 16 8571

(http://iopscience.iop.org/0953-8984/16/47/010)

INSTITUTE OF PHYSICS PUBLISHING JOURNAL OF PHYSICS: CONDENSED MATTER

J. Phys.: Condens. Matter **16** (2004) 8571–8588 PII: S0953-8984(04)85978-2

Formation of clusters in the ground state of the t–J model on a two-leg ladder

A Fledderjohann[1], A Langari[2,3,4] and K-H Mütter[1]

[1] Physics Department, University of Wuppertal, 42097 Wuppertal, Germany
[2] Institute for Advanced Studies in Basic Sciences, Zanjan 45195-1159, Iran
[3] Max-Planck-Institut für Physik komplexer Systeme, 01187 Dresden, Germany

E-mail: langari@mpipks-dresden.mpg.de

Received 8 September 2004
Published 12 November 2004
Online at stacks.iop.org/JPhysCM/16/8571
doi:10.1088/0953-8984/16/47/010

Abstract

We investigate the ground state properties of the t–J model on a two-leg ladder with anisotropic couplings $(t, \alpha = J/t)$ along rungs and $(t', \alpha' = J'/t')$ along legs. We have implemented a cluster approach based on four-site plaquettes. In the strong asymmetric cases $\alpha/\alpha' \ll 1$ and $\alpha'/\alpha \ll 1$ the ground state energy is well described by plaquette clusters with charges $Q = 2, 4$. The interaction between the clusters favours the condensation of plaquettes with maximal charge—a signal for phase separation. The dominance of $Q = 2$ plaquettes explains the emergence of tightly bound hole pairs. We have presented the numerical results from exact diagonalization to support our cluster approach.

1. Introduction: motivation and questions of interest

Since the discovery of high T_c superconductors [1]—almost twenty years ago—models of strongly correlated electron systems doped with holes have attracted much interest. The t–J model in two dimensions [2–9] and on ladders [10, 11] has been studied intensively in an effort to understand the behaviour of mobile holes in an antiferromagnetic background. Although some exact results in the special form of interactions exist [12, 13] the ground state and low energy excitations on the t–J ladder are not known exactly.

The generic mechanisms which explain the most striking features are of special interest, namely:

(i) the opening of a charge transfer gap [14],
(ii) the spatial separation of phases with hole rich and hole poor domains [15].

[4] Author to whom any correspondence should be addressed.

$H_1(N_1(\rho))$ H_{12} $H_2(N_2(\rho))$

$$N_1(\rho) = \frac{\rho_2 - \rho}{\rho_2 - \rho_1} N, \qquad N_2(\rho) = \frac{\rho - \rho_1}{\rho_2 - \rho_1} N$$

$$Q_1 = N_1(\rho)\rho_1, \qquad Q_2 = N_2(\rho)\rho_2$$

$$\psi(\rho_1, N_1(\rho)), \qquad \psi(\rho_2, N_2(\rho))$$

$$\varepsilon(\rho_1)N_1(\rho), \qquad \varepsilon(\rho_2)N_2(\rho)$$

Figure 1. Subdivision of a two-leg ladder.

Signatures of these features can be seen already in the ground state energy per site

$$\varepsilon(\rho) = \frac{E_{\mathrm{G}}}{N}, \qquad \rho = \frac{Q_{\mathrm{tot}}}{N}, \tag{1}$$

where E_{G}, N, Q_{tot} are the ground state energy, the number of sites and the total charge, respectively.

(i) A discontinuity in the first derivative, i.e. chemical potential,

$$\mu(\rho) = \frac{\mathrm{d}\varepsilon}{\mathrm{d}\rho}, \tag{2}$$

$$\mu(\rho) = \begin{cases} \mu_- & \rho \to \rho_0 - 0 \\ \mu_+ & \rho \to \rho_0 + 0, \end{cases} \tag{3}$$

signals the opening of a gap.
The inverse function

$$\rho(\mu) = \rho_0 \qquad \text{for } \mu_- \leqslant \mu \leqslant \mu_+, \tag{4}$$

develops a plateau with a width

$$\Delta = \mu_+ - \mu_-, \tag{5}$$

which is related to the charge transfer gap. This is quite analogous to the plateaux in the magnetization curve $M = M(B)$, which are related to the spin gap.

(ii) A linear behaviour of $\varepsilon(\rho)$ in some interval, $\rho_1 \leqslant \rho \leqslant \rho_2$:

$$\varepsilon_L(\rho) = \frac{1}{\rho_2 - \rho_1} \left[\varepsilon(\rho_1)(\rho_2 - \rho) + \varepsilon(\rho_2)(\rho - \rho_1)\right], \tag{6}$$

signals the spatial separation of two phases: the first one with charge density ρ_1, the second one with ρ_2.
For demonstration, let us consider a two-leg ladder, which we divide into two parts with sites N_j, charges Q_j, Hamiltonians H_j, ground state wavefunctions $\psi(\rho_j, N_j)$ and ground state energies $\varepsilon(\rho_j)N_j(\rho)$ as illustrated in figure 1.
The Hamiltonian of the whole ladder

$$H = H_1(N_1(\rho)) + H_2(N_2(\rho)) + H_{12} \tag{7}$$

contains in addition an interaction term, which is mediated via the two (dashed) links connecting the subladders. Each bond in figure 1 corresponds to the usual t–J Hamiltonian, composing of an electron hopping term $t(c^{\dagger}_{i,\sigma}c_{j,\sigma}+c^{\dagger}_{j,\sigma}c_{i,\sigma})$ and an exchange interaction $J(S_i \cdot S_j - n_i n_j/4)$. The elimination of doubly occupied states has been also imposed. The indices i, j refer to nearest neighbour sites, σ to electron spin and the couplings on legs are defined as (t', J').

The product ansatz

$$\psi(\rho, N) = \psi(\rho_1, N_1(\rho))\psi(\rho_2, N_2(\rho)) \tag{8}$$

describes a state with charge density ρ and two spatially separated phases, the first one with charge density ρ_1 and $N_1(\rho)$ sites and the second with charge density ρ_2 and $N_2(\rho)$ sites. If we estimate the expectation value of the Hamiltonian (7) with the variational ansatz (8), we get an upper bound

$$\varepsilon(\rho) \leqslant \varepsilon_L(\rho) \qquad \text{for } \rho_1 \leqslant \rho \leqslant \rho_2, \tag{9}$$

in terms of the right-hand side of (6).

Note that the interaction term

$$\frac{1}{N}\langle\psi(\rho)|H_{12}|\psi(\rho)\rangle,$$

does not survive in the thermodynamical limit $N \to \infty$. Since (9) is a strict upper bound in the thermodynamical limit for any interval

$$\rho_1 \leqslant \rho \leqslant \rho_2,$$

we can conclude that $\varepsilon(\rho)$ is a convex function of ρ. The product ansatz (8) with the two separated phases represents the true ground state if the upper bound (9) holds sharply. In this case, we derive from (6) a constant chemical potential:

$$\mu = \frac{\mathrm{d}\varepsilon}{\mathrm{d}\rho} = \frac{\varepsilon(\rho_2) - \varepsilon(\rho_1)}{\rho_2 - \rho_1} = \mu_0 \qquad \text{for } \rho_1 \leqslant \rho \leqslant \rho_2, \tag{10}$$

which corresponds to a discontinuity in the inverse function

$$\rho(\mu) = \begin{cases} \rho_1 & \text{for } \mu \to \mu_0 + 0 \\ \rho_2 & \text{for } \mu \to \mu_0 - 0. \end{cases} \tag{11}$$

It is the purpose of this paper to demonstrate that the generic mechanisms, which lead to gaps and phase separations, are intimately related to the formation of clusters. On ladder systems the formation of clusters is prescribed in a natural way by the ladder geometry.

It is plausible to start with the simplest clusters, defined by the rungs. In the limit of vanishing hopping parameter t' along the legs, the system decouples into a product of rung eigenstates. This limit has been studied intensively in the literature under various descriptions such as the 'local rung approximation' [16] or 'bond operator theory' [17]. In [19], we studied first-order corrections in the leg hopping parameter t' and compared perturbative results with exact diagonalizations on a 2×8 ladder for parameter values

$$\begin{aligned} &t = 1, \qquad \alpha = J = 0.5, \\ &t' = 0.1, 0.2, 0.3, \qquad \alpha' = J'/t' = 2.7. \end{aligned} \tag{12}$$

As regards the quality of the perturbation expansion based on the local rung approximation we found

- good agreement in the regime $0 \leqslant \rho \leqslant 1/2$,
- failure in the regime $1/2 \leqslant \rho \leqslant 1$.

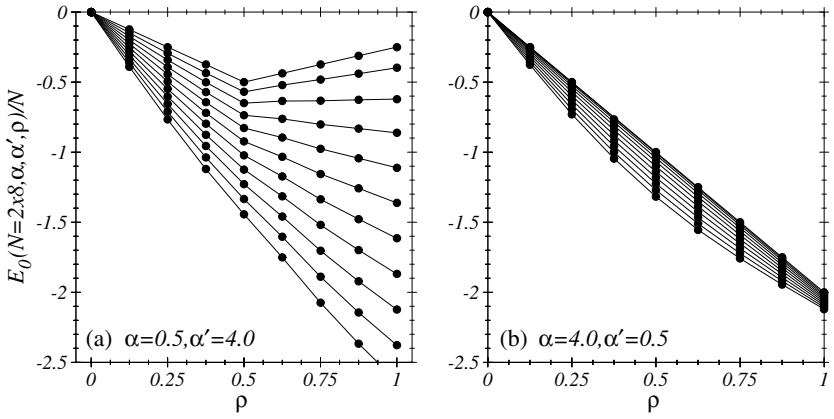

Figure 2. Lanczos results for energies per site of an $N = 2 \times 8$ t–J ladder for the parameters (15a), (15b). For both cases shown, t' increases from top to bottom as $t' = 0, 0.1, \ldots, 1.0$.

We do not think that higher orders in perturbation expansion with local rungs will improve the situation in the second regime. Instead we are convinced that the starting point—i.e. the clusters which define the zeroth-order perturbation theory—has to be changed.

In this paper we intend to demonstrate, on the two-leg ladder with anisotropic couplings, how the appropriate clusters which define the zeroth-order perturbation theory are to be found. We start in section 2 with an analysis of the exact ground state energy per site $\varepsilon(\rho)$ on a 2×8 ladder (cf figures 2(a), (b)) which turns out to be almost linear in the charge density ρ for an appropriate choice of the system parameters (equations (15a) and (15b)). As explained above, the linearity in ρ indicates phase separation into two clusters with charge densities

$$\rho_1 = 0 \qquad \rho_2 = \tfrac{1}{2} \qquad \text{for } 0 \leqslant \rho \leqslant \tfrac{1}{2}, \tag{13}$$

$$\rho_1 = \tfrac{1}{2} \qquad \rho_2 = 1 \qquad \text{for } \tfrac{1}{2} \leqslant \rho \leqslant 1. \tag{14}$$

The dependence of the ground state energy per site (6) on the system parameters is very well reproduced by the plaquette ground state energies $E^{(\mathrm{p})}(Q)$ with plaquette charges $Q = 2, 4$.

In section 3 we present the perturbation expansion based on plaquette clusters. First-order corrections, which describe the interaction between neighbouring plaquettes, favour the clustering of plaquettes with charges $Q = 4$—a first indication of phase separation.

In section 4 we investigate in which circumstances plaquette clusters with odd charges $Q = 1$ and 3 are suppressed energetically.

In the low doping case $\rho > 3/4$ the dominance of $Q = 2$ and suppression of $Q = 3$ plaquettes in the ground state explains the emergence of tightly bound hole pairs [18] for an appropriate choice of the rung and leg couplings. Finally, a discussion on our results will be presented.

2. Approximate linear charge density dependence of the ground state energy

We start in figures 2(a), (b) with Lanczos results on the ground state energy per site in the t–J model with anisotropic couplings $t, \alpha = J/t$ (throughout this paper we have chosen $t \equiv 1$), $t', \alpha' = J'/t'$ for the rungs and legs respectively on a 2×8 ladder:

$$\alpha = 0.5, \qquad \alpha' = 4.0, \qquad t' = 0, 0.1, \ldots, 1.0, \tag{15a}$$

$$\alpha = 4.0, \qquad \alpha' = 0.5, \qquad t' = 0, 0.1, \ldots, 1.0. \tag{15b}$$

There is a pronounced difference between the dependences on ρ of the ground state energies in figures 2(a) and (b). In figure 2(a) we observe a discontinuity in the slope $\mu(\rho) = \mathrm{d}\varepsilon/\mathrm{d}\rho$ at $\rho = 1/2$, which generates a plateau in the charge density $\rho(\mu)$ as function of the chemical potential:

$$\rho(\mu) = \tfrac{1}{2} \qquad \mu_- \leqslant \mu \leqslant \mu_+. \tag{16}$$

The plateau width

$$\Delta = \mu_+ - \mu_- \tag{17}$$

shrinks with increasing values of t'. Note also that the chemical potential $\mu(\rho) = \mathrm{d}\varepsilon/\mathrm{d}\rho$ vanishes for $\rho > 1/2$ for a specific value of $t' = t'_0(\alpha, \alpha')$. This feature will be discussed in section 4.

Let us next turn to the ground state energy $\varepsilon(\rho)$ in the domain (15b) shown in figure 2(b). At $t' = 0$, there is no discontinuity in the slope—i.e. no plateau in $\rho(\mu)$—at $\rho = 1/2$. The variation with the leg hopping parameter t' is much smaller than in case (a). For $t' > 0$, $\varepsilon(\rho, t')$ is only approximately linear in the two subintervals $0 \leqslant \rho \leqslant 1/2$ and $1/2 \leqslant \rho \leqslant 1$ with different slopes μ_- and μ_+. The difference $\Delta = \mu_+ - \mu_-$ increases with t'. Deviations from linearity are convex as predicted by (9).

The product ansatz (8) describes a system with two phases:

For $0 \leqslant \rho \leqslant 1/2$ with a ground state energy

$$\varepsilon(\rho, t') = \varepsilon(0, t')(1 - 2\rho) + \varepsilon(1/2, t')2\rho \tag{18}$$

there is a phase with charge density $\rho_1 = 0$ in the first part of the ladder and a second phase with charge density $\rho_2 = 1/2$ in the second part. Phase separation occurs at $N_1(\rho) = (1 - 2\rho)N$.

For $1/2 \leqslant \rho \leqslant 1$ with a ground state energy

$$\varepsilon(\rho, t') = 2\varepsilon(1/2, t')(1 - \rho) + \varepsilon(1, t')(2\rho - 1) \tag{19}$$

the two phases in the first and second part of the ladder have charge densities $\rho_1 = 1/2$ and $\rho_2 = 1$, respectively. Here the phase separation occurs at $N_1(\rho) = 2(1 - \rho)N$.

For $0 \leqslant \rho \leqslant 1/2$ the dependence of $\varepsilon(\rho, t')$ (18) on the parameters t', α, α' only enters via $\varepsilon(1/2, t', \alpha, \alpha')$. Results on a 2×8 ladder are shown for this quantity in figures 3(a) and (b) with the parameter choices

$$\alpha = 0.4, 0.5, 0.6, \qquad \alpha' = 4.0, 5.0, 6.0, \qquad t' = 0, 0.1, \ldots, 1.0, \tag{20a}$$

$$\alpha = 4.0, 5.0, 6.0, \qquad \alpha' = 0.4, 0.5, 0.6, \qquad t' = 0, 0.1, \ldots, 1.0. \tag{20b}$$

It turns out that the whole dependence on the parameters t', α, α':

$$\varepsilon(1/2, t', \alpha, \alpha') = \tfrac{1}{4} E^{(\mathrm{p})}(2, t', \alpha, \alpha') f(1/2, t', \alpha, \alpha'), \tag{21}$$

is correctly reproduced by the (2×2) plaquette ground state energies $E^{(\mathrm{p})}(Q, t', \alpha, \alpha')$ with charge $Q = 2$ up to a correction factor $f(1/2, t', \alpha, \alpha')$. The physical interpretation of f is given below.

As is shown in appendix A (cf (A.13)–(A.18)), we have different ground states in the regimes (20a) and (20b) for plaquettes with charge $Q = 2$. The ground state energies follow from the lowest eigenvalues of the 3×3 matrix (A.9), which are computed in a perturbation expansion with zeroth-order contributions (A.15) and (A.18) for the regimes (20a) and (20b):

$$E^{(P)}_{(a)}(2, t', \alpha, \alpha') = -\tfrac{1}{2}\left(J' + \sqrt{J'^2 + 16}\right), \tag{22a}$$

$$E^{(P)}_{(b)}(2, t', \alpha, \alpha') = -\tfrac{1}{2}\left(\alpha + \sqrt{\alpha^2 + 16t'^2}\right). \tag{22b}$$

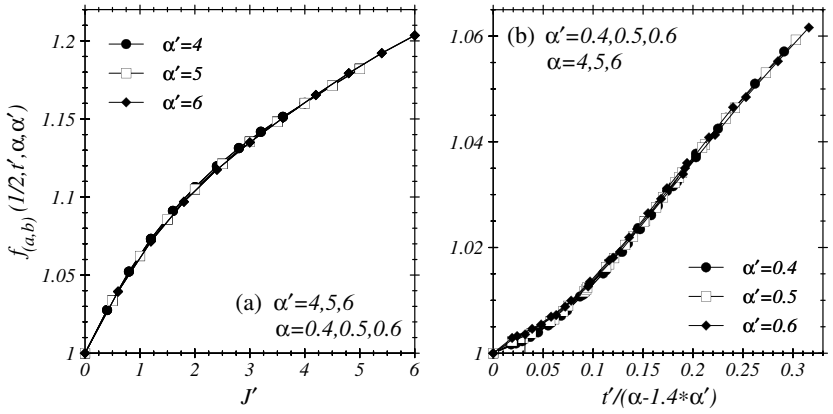

Figure 3. The correction factor $f(1/2, t', \alpha, \alpha')$ of (21) for a 2×8 t–J ladder with parameters (20a), (20b) and $\rho = 1/2$.

In figures 3(a) and (b) we have plotted the correction factors in (21):

$$f_{(a)}(1/2, t', \alpha, \alpha') = f_{(a)}(1/2, J' = \alpha' t'), \tag{23a}$$

$$f_{(b)}(1/2, t', \alpha, \alpha') = f_{(b)}(1/2, t'/(\alpha - 1.4\alpha')). \tag{23b}$$

versus the 'scaling variables' $J' = \alpha' t'$ and $t'/(\alpha - 1.4\alpha')$, respectively. Note, that all data points for (20a) and (20b) almost coincide if we use the scaling variables.

Let us next discuss the linear behaviour with ρ in (19). The dependence on the parameters t', α, α' enters via $\varepsilon(1/2, t', \alpha, \alpha')$ ((21), (22a), (22b)) and $\varepsilon(1, J = \alpha, J' = \alpha' t')$. Note that for $\rho = 1$, $\varepsilon(1, J, J')$ is just the ground state energy per site of the spin 1/2 Heisenberg model on a two-leg ladder with spin couplings J and J' along the rungs and legs, respectively[5]. The J, J' dependence

$$\varepsilon(1, J, J') = \tfrac{1}{4} E^{(\mathrm{p})}(4, J, J') f(1, J'/J), \tag{24}$$

is correctly reproduced by the plaquette ground state energy $E^{(\mathrm{p})}(Q, J, J')$ with charge $Q = 4$ (cf (A.28)):

$$E^{(\mathrm{p})}(Q = 4, J, J') = -J - J' - \sqrt{J^2 + J'^2 - JJ'}, \tag{25}$$

up to a correction factor $f(1, J'/J)$, which is shown in figures 4(a), (b) and which scales in J'/J.

3. Plaquette clusters in the ground state of the t–J model on a two-leg ladder

The results of the numerical analysis in the last section motivate us to build up the ground state on the two-leg ladder from plaquette eigenstates.

For this purpose the t–J Hamiltonian

$$H = t \sum_{j=1}^{N/4} h_{j,j}(t', \alpha', \alpha) + t'' \sum_{j=1}^{N/4-1} h_{j,j+1}(\alpha'') \tag{26}$$

[5] Note that at $\rho = 1$ the Heisenberg and t–J Hamiltonians are differing by a constant diagonal contribution $(-1/4)$ per bond.

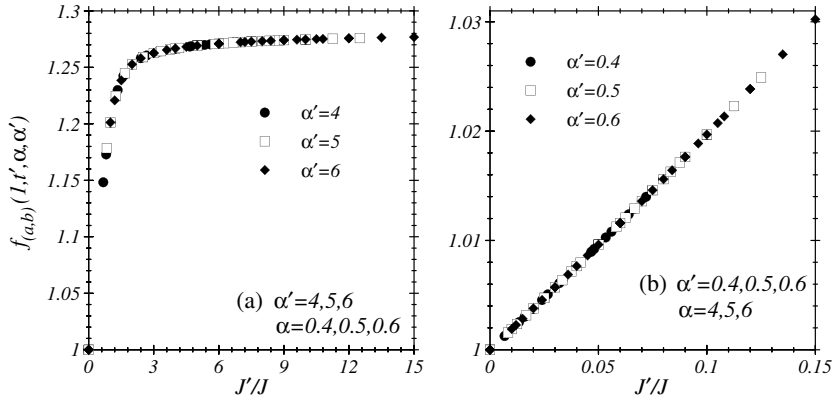

Figure 4. The correction factor $f(1, t', \alpha, \alpha')$ of (24) for a 2×8 t–J ladder with parameters (20a), (20a) and $\rho = 1$.

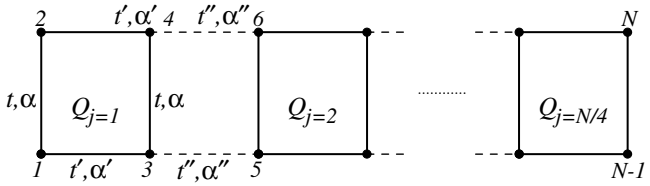

Figure 5. Decomposition of the two-leg t–J ladder into coupled (t'', α'') four-site plaquette clusters.

is decomposed into $N/4$ plaquette Hamiltonians (using the notation of [19])

$$h_{j,j}(t', \alpha', \alpha) = \frac{t'}{t}[h(4j-3, 4j-1, \alpha') + h(4j-2, 4j, \alpha')] + [h(4j-3, 4j-2, \alpha) + h(4j-1, 4j, \alpha)], \tag{27}$$

with spin couplings $J = t\alpha$, $J' = t'\alpha'$ and hopping terms t, t' along the rungs and legs, respectively (cf figure 5).

$$h_{j,j+1}(\alpha'') = h(4j-1, 4j+1, \alpha'') + h(4j, 4j+2, \alpha'') \tag{28}$$

describes the interaction between neighbouring plaquettes j, $j+1$. This interaction is treated in the following in a perturbative expansion around $t'' = 0$, $J'' = 0$, $\alpha' = \alpha'' = J''/t''$ fixed. In the analysis of the numerical results for the ground state energies (21) and (24) at $\rho = 1/2$ and $\rho = 1$, this interaction generates the correction factors $f(\rho = 1/2)$ and $f(\rho = 1)$—shown in figures 3(a), (b) and 4(a), (b) respectively.

The lowest plaquette eigenstates

$$h_{j,j}(t', \alpha', \alpha)\psi^{(\mathrm{p})}_{n_j}(Q_j) = E^{(\mathrm{p})}_{n_j}(Q_j)\psi^{(\mathrm{p})}_{n_j}(Q_j), \tag{29}$$

in the sector with charge $Q_j = 0, 2, 4$, $Q_j = 1, 3$ and total plaquette spin 0 and 1/2, respectively, are discussed in appendix A. The eigenstates $\psi^{(\mathrm{p})}_{n_j=0}(Q_j) = \psi^{(\mathrm{p})}(Q_j)$ with lowest energy $E^{(\mathrm{p})}_{n_j=0}(Q_j) = E^{(\mathrm{p})}(Q_j)$ yield the basis for the ground state on the two-leg ladder in lowest order perturbation theory $t'' = 0$.

To zeroth order in t'' ($t'' = 0$) the eigenstates of the Hamiltonian (26) are given by a product of plaquette ground states $\psi^{(\mathrm{p})}(Q_j)$

$$\prod_{j=1}^{N/4} \psi^{(\mathrm{p})}(Q_j), \tag{30}$$

with energies

$$E_n = \sum_{j=1}^{N/4} E^{(\mathrm{p})}(Q_j). \tag{31}$$

The plaquette charges Q_j have to add up to the total charge:

$$Q_{\mathrm{tot}} = \sum_j Q_j. \tag{32}$$

Our analysis in section 2 suggests that only plaquette ground states with charges $Q = 0, 2, 4$:

$$\psi^{(\mathrm{p})}(0), \psi^{(\mathrm{p})}(2) \qquad \text{for } 0 \leqslant \rho \leqslant 1/2, \tag{33}$$

$$\psi^{(\mathrm{p})}(2), \psi^{(\mathrm{p})}(4) \qquad \text{for } 1/2 \leqslant \rho \leqslant 1, \tag{34}$$

are involved in the construction of the ground state of the two-leg ladder. The corresponding ground state energies on the ladder:

$$E(\rho, t', \alpha', \alpha, t'' = 0) = N^{(i)}(i) E_0^{(\mathrm{p})}(Q = i) + N^{(i)}(i+2) E_0^{(\mathrm{p})}(Q = i+2), \tag{35}$$

$$i = 0 \qquad \text{for } 0 \leqslant \rho \leqslant 1/2,$$
$$i = 2 \qquad \text{for } 1/2 \leqslant \rho \leqslant 1,$$

are obtained from plaquette ground state energies $E^{(\mathrm{p})}(Q)$ and the number $N^{(i)}(Q)$ of plaquettes with charge Q:

$$N^{(0)}(0) + N^{(0)}(2) = N^{(2)}(2) + N^{(2)}(4) = N/4, \tag{36}$$

$$2N^{(0)}(2) = 2N^{(2)}(2) + 4N^{(2)}(4) = Q_{\mathrm{tot}}. \tag{37}$$

So far we have only treated the zeroth-order perturbation theory (26) ($t'' = 0$). The product states are degenerate since the $N^{(i)}(Q)$ plaquettes with charges $Q = 0$, $Q = 2$ for $i = 0$ and $Q = 2$, $Q = 4$ for $i = 2$ can be distributed in different ways over the ladder (figure 5).

The interaction energy $W(Q_j, Q_{j+1})$ between neighbouring plaquettes is derived in appendix B in the framework of a first-order perturbation theory in the hopping parameter t''. The resulting shift ΔE in the ground state energy:

$$\Delta E^{(0)} = N^{(0)}(2,2) W(2,2) \qquad \text{for } i = 0, \quad 0 \leqslant \rho \leqslant 1/2; \tag{38}$$

$$\Delta E^{(2)} = N^{(2)}(2,2) W(2,2) + N^{(2)}(2,4) W(2,4) + N^{(2)}(4,4) W(4,4)$$
$$\text{for } i = 2, \quad 1/2 \leqslant \rho \leqslant 1 \tag{39}$$

can be expressed in terms of the interaction energies $W(Q_j, Q_{j+1})$ and numbers $N(Q_j, Q_{j+1})$ of neighbouring plaquettes with charges Q_j, Q_{j+1}. Since $W(0,0) = W(0,2) = 0$ and $W(2,2) = -J'/8$ (B.7), $\Delta E^{(0)}$ is minimal if $N^{(0)}(2,2)$ is maximal:

$$N^{(0)}(2,2) = N^{(0)}(2) - 1 = \frac{N}{2}\rho - 1, \tag{40}$$

According to (B.7),

$$W(2,2) + W(4,4) - 2W(2,4) < 0. \tag{41}$$

Table 1. Results for $J'(J)$ and $\varepsilon(\rho, J' = J'(J))$ for rung spin exchange couplings $J = \alpha = 0.4, 0.5, 0.6$ on the basis of (46) and (49).

$J = \alpha$	0.4	0.5	0.6
$J' = J'(J)$	0.948 95	0.888 39	0.812 55
$\varepsilon(\rho, J'(J))$	−0.662 15	−0.650 99	−0.637 17

$\Delta E^{(2)}$ is minimal if $N^{(2)}(4, 4)$ (and thereby $N^{(2)}(2, 2)$) are maximal:

$$N^{(2)}(4, 4) = N^{(2)}(4) - 1 = \frac{N}{2}(\rho - 1/2) - 1, \tag{42}$$

$$N^{(2)}(2, 2) = N^{(2)}(2) - 1 = \frac{N}{2}(1 - \rho) - 1, \tag{43}$$

$$N^{(2)}(2, 4) = 1. \tag{44}$$

The perturbative result on the ground state energy per site in the regime (20*a*)

$$\varepsilon(\rho) = (1 - \rho)\tfrac{1}{2}(E^{(\mathrm{p})}(2) + W(2, 2)) + \tfrac{1}{2}(\rho - 1/2)(E^{(\mathrm{p})}(4) + W(4, 4)), \tag{45}$$

predicts a level crossing in all charge sectors with $1/2 < \rho < 1$ if

$$E^{(\mathrm{p})}(4) - E^{(\mathrm{p})}(2) + W(4, 4) - W(2, 2) = 0. \tag{46}$$

In the regime (20*a*) the left-hand side with (25), (22*a*) and

$$W(4, 4) - W(2, 2) = -\tfrac{3}{8}J' \tag{47}$$

only depends on J, J'. The solution defines a curve $J' = J'(J)$ in the parameter space, where the ground state energy (45) becomes independent of ρ; the corresponding chemical potential

$$\mu = \frac{\mathrm{d}\varepsilon}{\mathrm{d}\rho} = 0 \qquad \text{for } 1/2 \leqslant \rho \leqslant 1 \quad \text{and} \quad J' = J'(J), \tag{48}$$

turns out to be zero here.

Moreover, the ground state energy along the curve $J'(J)$ is predicted to be

$$\varepsilon(\rho, J' = J'(J)) = \frac{1}{4}E_0^{(\mathrm{p})}(2) - \frac{J'}{32}. \tag{49}$$

Results for $J'(J)$ and $\varepsilon(\rho, J' = J'(J))$ are given in table 1.

As an illustration, we present in figure 6 the ground state energy per site $\varepsilon(\rho, t', \alpha') = E(N, Q, t', \alpha', \alpha = 1/2)/N$ for the charges $Q = 8, 10, \ldots, 16$ at $\alpha = 0.5$, $\alpha' = 4.0$ (a) and $\alpha' = 2.7$ (b).

The crossing of these energy levels at

$$t_0' = \frac{J'(J = 0.5)}{\alpha'} = \begin{cases} 0.222 & \text{for } \alpha' = 4.0 \\ 0.329 & \text{for } \alpha' = 2.7, \end{cases} \tag{50}$$

is predicted to change with α' if we keep $\alpha = J = 0.5$ fixed. On the other hand, the corresponding ground state energy per site

$$\varepsilon(\rho, J'(J = 0.5)) = -0.650\,99, \tag{51}$$

is independent of α'!

Both predictions (50) and (51) are clearly visible in the numerical results on a 2×8 ladder.

We also looked for level crossings (46) in the regime (20*b*). It turns out that they occur at t' values $t'' = t' > 1$, where the perturbative approach is not reliable.

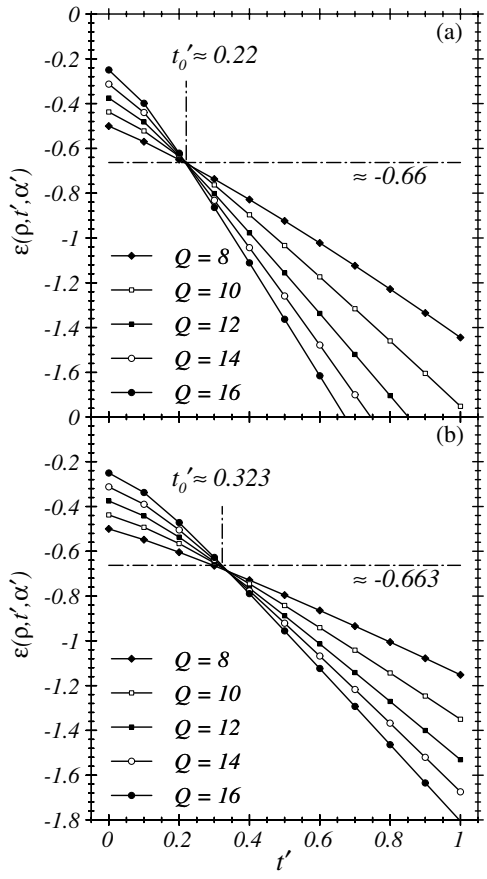

Figure 6. Lanczos results for the crossing of energy levels for $\rho = Q/N \geqslant 1/2$ and $\alpha = 0.5$, $\alpha' = 4.0$ (a), $\alpha' = 2.7$ (b) for an $N = 2 \times 8$ t–J ladder.

4. The special role of plaquette clusters with charges $Q = 2$ and 4

The variational ansatz (30) with plaquette clusters only involves cluster eigenstates (33), (34) with even charges $Q = 0, 2, 4$. Such an ansatz makes sense if plaquette clusters with odd charges are suppressed energetically:

$$\Delta_1 = E^{(\mathrm{p})}(0) + E^{(\mathrm{p})}(2) - 2E^{(\mathrm{p})}(1) < 0, \tag{52}$$

$$\Delta_3 = E^{(\mathrm{p})}(2) + E^{(\mathrm{p})}(4) - 2E^{(\mathrm{p})}(3) < 0. \tag{53}$$

In appendix A we discuss the low lying eigenstates of plaquette clusters with charges $Q = 0, 1, 2, 3, 4$. The ground state energies for $Q = 0, 1, 4$ are unique in the sense that there are no level crossings by variation of the parameters t', α', α. The ground state energy of the $Q = 2$ cluster is given by (22*a*) and (22*b*).

It turns out that the inequalities (52) and (53) are indeed satisfied in the regimes (15*a*) and (15*b*), respectively.

The suppression of $Q = 3$ plaquettes in the regime (53) has immediate consequences for the mobility and correlations of holes as they are discussed by Siller *et al* [18] for the low doping case ($\rho > 3/4$). In the regime $\Delta_3 < 0$, hole pairs are confined in $Q = 2$ plaquettes and

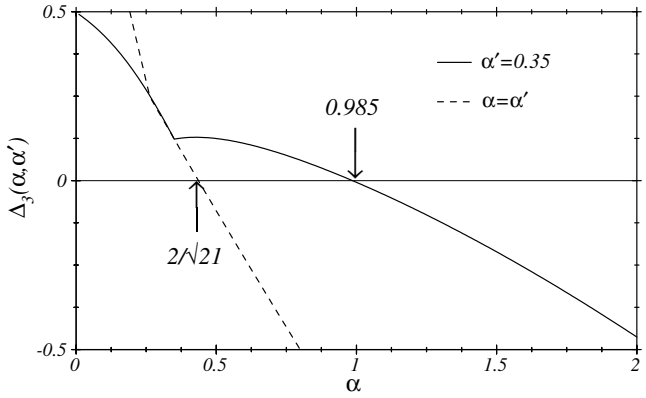

Figure 7. Energy differences $\Delta_3(\alpha, \alpha')$ for (1) $\alpha' = 0.35$ and (2) $\alpha = \alpha'$ (in both cases, $t = t' = 1$).

cannot move in the antiferromagnetic background of the $Q = 4$ plaquettes. This can be seen in the first-order perturbation theory (cf appendix B) for the interaction between neighbouring plaquettes, which forbids the transition

$$Q_j = 2 \qquad Q_{j+1} = 4 \rightarrow Q'_j = 4 \qquad Q'_{j+1} = 2, \tag{54}$$

with charge transfer $\Delta Q = 2$. Therefore the hopping of the hole pair confined in the $Q = 2$ plaquette is suppressed in the antiferromagnetic background.

On the other hand, hopping of a single hole contained in a plaquette with $Q = 3$ is possible since the transition

$$Q_j = 3 \qquad Q_{j+1} = 4 \rightarrow Q'_j = 4 \qquad Q'_{j+1} = 3 \tag{55}$$

is not forbidden.

It is interesting to study the energy difference $\Delta_3(\alpha, \alpha')$ for the α, α' values of [18]. There the leg coupling $\alpha' = J'/t'$ has been chosen to be $\alpha' = 0.35$ whereas the rung coupling varies: $\alpha \geqslant \alpha' = 0.35$. The hopping parameters are equal: $t = t'$. For large $\alpha > 4$ this corresponds to our regime (20*b*).

In figure 7 we have plotted the difference $\Delta_3(\alpha, \alpha' = 0.35)$. For comparison we have also included the difference $\Delta_3(\alpha = \alpha')$ with symmetric couplings along the rungs and legs, respectively. The latter drops monotonically with $\alpha = \alpha'$ and is zero at

$$\alpha = \alpha' = \frac{2}{\sqrt{21}} = 0.436\ldots. \tag{56}$$

In contrast, the difference $\Delta_3(\alpha, \alpha' = 0.35)$ in the asymmetric case $\alpha > \alpha' = 0.35$ first increases and has a flat maximum at $\alpha \simeq 0.43$ and then drops, with a zero at

$$\Delta_3(\alpha \simeq 0.985, \alpha' = 0.35) = 0. \tag{57}$$

The zeros (56) and (57) of Δ_3 mark the transition where $Q = 3$ plaquettes are replaced by $Q = 2$ plaquettes and two holes combine to a pair. We expect that the hole–hole correlation length has a maximum at this transition point. Indeed there is a maximum of the hole–hole correlation length at $\alpha = 1.2$, as determined in [18] from a DMRG calculation on a 40×2 ladder. It might be accidental that the value $\alpha = 1.2$ is quoted as well as a lower bound for phase separation in the 2D t–J model with isotropic couplings [5]. We therefore calculated (53) also for the isotropic case $\alpha = \alpha'$, where the zero (56) is formed quite far below $\alpha = 1.2$.

It would be interesting to see whether the maximum of the correlation length is shifted also to a smaller value in the symmetric case $\alpha = \alpha'$.

We are aware of the fact that our considerations in the low doping regime ($\rho > 3/4$) are based on the product ansatz (30) with plaquette clusters with charges

$$Q = 2, 4 \qquad \text{for } \Delta_3 < 0, \tag{58}$$

$$Q = 3, 4 \qquad \text{for } \Delta_3 > 0. \tag{59}$$

The interaction between neighbouring plaquettes is neglected. This is justified for (58) if Δ_3 is sufficiently negative, as was demonstrated in sections 2 and 3. On the other hand, these interactions cannot be neglected in the regime (59) where first-order perturbation theory allows the hopping (55) of $Q = 3$ plaquettes in the antiferromagnetic background of $Q = 4$ plaquettes. In this case, first-order perturbation theory leads to an effective Hamiltonian on a chain with nearest neighbour couplings. The effective degrees of freedom at each site and their nearest neighbour interactions are defined by the ground states of the $Q = 3$ and 4 plaquettes. We expect that such an effective Hamiltonian will induce a convex curvature in the dependence on ρ of the ground state energy, which would indicate that we are beyond the phase separated phase. We observed this curvature (for $0 < \rho < 1/2$) with an effective Hamiltonian based on rung clusters and their interactions [19].

5. Discussion and perspectives

The formation of clusters in the ground state of a quasi-one-dimensional system has important consequences for its physical properties, e.g. the phase diagram at zero temperature.

In case of the t–J model on a two-leg ladder with asymmetric couplings ($\alpha = J/t, \alpha' = J'/t'$; regime (20*a*) $\alpha/\alpha' \ll 1$ and regime (20*b*) $\alpha/\alpha' \gg 1$) plaquette clusters with even charges $Q = 0, 2, 4$ play the dominant role and explain the charge density and (α, α', t') dependence of the ground state energies, as was demonstrated in sections 3 and 4. First-order perturbation theory for the interaction of neighbouring plaquettes favours the condensation of plaquettes with the same charge ($Q = 2, 4$), which can be interpreted as a signal for phase separation. Of course, this can happen only if plaquette clusters with odd charges $Q = 1, 3$ are suppressed energetically, which means that the energy combinations (52) and (53) are sufficiently negative.

The low doping regime ($\rho \geqslant 3/4$) is of special interest. It has been demonstrated in [18] that the hole–hole correlations are small in the t–J model with asymmetric couplings on legs ($\alpha' = 0.35$) and rungs ($\alpha > 4$). In this regime the ground state is very well described with plaquette clusters of charge $Q = 2, 4$. The $Q = 4$ plaquettes generate the antiferromagnetic background. In each $Q = 2$ plaquette a pair of holes is confined. The holes can be deconfined only if the resulting two plaquettes with charge $Q = 3$ are energetically preferred (cf (53) for $\Delta_3 > 0$). As was demonstrated in section 4 this happens for smaller α values ($\alpha' = 0.35 < \alpha < 0.98$ in the asymmetric case, $\alpha = \alpha' < 2/\sqrt{21}$ in the symmetric case). In this regime the ground state is more complex [18] and can be modelled by 'hard core bosons'.

In our approach based on a product ansatz with clusters we have two possibilities for exploiting the ground state in this regime: (A) We compute the effective Hamiltonian which describes the interaction between $Q = 3$ and 4 plaquettes perturbatively. (B) We improve the quality of the product ansatz with larger clusters such that hole–hole correlations at larger distances are properly taken into account as well.

Acknowledgment

We are indebted to A Klümper for a critical reading of the manuscript.

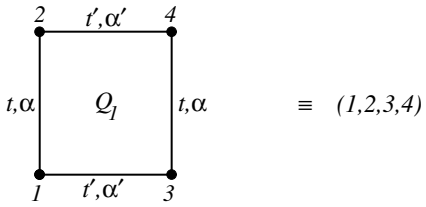

Figure A.1. The notation and shape of the four-site cluster used—the building block for the two-leg t–J ladder.

Appendix A. Eigenstates of the four-site cluster

The Hamiltonian of the four-site cluster (cf figure A.1) is defined in (26) (for $j = 1$).

We are now going to construct all $N_c(Q)$ eigenstates for cluster charges $Q = Q_1 = 0, 1, 2, 3, 4$—assuming equal numbers of spin-up (+) and spin-down (−) charges for even Q and an excess of one spin-up particle for odd cluster charges Q. Moreover, we will assume $t, J, t', J' \geqslant 0$.

The difference in coupling parameters for rungs (t, J) and legs (t', J') subdivides the basis states for each Q into the classes $\{|\mathrm{III}\rangle\}$ and $\{|\mathrm{I}\rangle, |\mathrm{II}\rangle\}$:

$$\begin{array}{lcccc} & Q=1 & Q=2 & Q=3 & Q=4 \\ |\mathrm{III}\rangle: & \left|\begin{matrix}0&0\\+&0\end{matrix}\right\rangle, & \left|\begin{matrix}0&-\\+&0\end{matrix}\right\rangle, & \left|\begin{matrix}+&0\\-&+\end{matrix}\right\rangle, & \left|\begin{matrix}-&+\\+&-\end{matrix}\right\rangle, \\ & \left|\begin{matrix}+&0\\0&0\end{matrix}\right\rangle, & \left|\begin{matrix}+&0\\0&-\end{matrix}\right\rangle, & \left|\begin{matrix}-&+\\+&0\end{matrix}\right\rangle, & \left|\begin{matrix}+&-\\-&+\end{matrix}\right\rangle, \end{array} \tag{A.1}$$

and[6]

$$|\mathrm{I}\rangle: \left|\begin{matrix}-&0\\+&0\end{matrix}\right\rangle, \left|\begin{matrix}-&0\\+&+\end{matrix}\right\rangle, \left|\begin{matrix}-&-\\+&+\end{matrix}\right\rangle, \left|\begin{matrix}+&0\\-&0\end{matrix}\right\rangle, \left|\begin{matrix}+&+\\-&0\end{matrix}\right\rangle, \tag{A.2}$$

$$|\mathrm{II}\rangle: \left|\begin{matrix}0&0\\+&-\end{matrix}\right\rangle, \left|\begin{matrix}+&0\\+&-\end{matrix}\right\rangle, \left|\begin{matrix}+&-\\+&-\end{matrix}\right\rangle, \left|\begin{matrix}0&0\\-&+\end{matrix}\right\rangle, \left|\begin{matrix}+&-\\+&0\end{matrix}\right\rangle, \tag{A.3}$$

as regards the behaviour with respect to transformations

$$\hat{R}: \quad (1, 2, 3, 4) \longrightarrow (1, 3, 2, 4), \tag{A.4}$$

i.e. the interchange of legs and rungs.

(a) $Q = 0$, $N_c(0) = 1$

$$E^{(\mathrm{p})}(Q = 0) = 0. \tag{A.5}$$

(b) $Q = 1$, $N_c(1) = 4$

We introduce $|n\rangle$ as the $Q = 1$ basis state with the spin-up particle (+) at plaquette position n ($|n\rangle \equiv c^{+}_{n\uparrow}|0\rangle$).

[6] Note that each state shown represents two elements due to successive rotations by π—except for the $Q = 4$ states in (A.1).

Using the basis

$$|1,\tau,\zeta\rangle = \tfrac{1}{2}[(|1\rangle + \tau|4\rangle) + \zeta(|2\rangle + \tau|3\rangle)] \tag{A.6}$$

with $\tau = \pm 1$, $\zeta = \pm 1$, we obtain the eigenvalues

$$E^{(\mathrm{p})}(Q=1,\tau,\zeta) = -\zeta(t + \tau t'). \tag{A.7}$$

(c) $Q = 2$, $N_{\mathrm{c}}(2) = 12$

Introducing $|m,n\rangle$ as the $Q = 2$ basis state with spin-up particles (+) at site m and (−) at position n ($|m,n\rangle \equiv c^{+}_{m\uparrow}c^{+}_{n\downarrow}|0\rangle$), we first compute the action of the t–J Hamiltonian on the singlet ($\tau = 1$) and triplet states ($\tau = -1$):

$$\begin{aligned}
|1,(\tau,\zeta)\rangle &= [|1,2\rangle + \tau|2,1\rangle + \zeta\,(|3,4\rangle + \tau|4,3\rangle)]/2,\\
|2,(\tau,\zeta)\rangle &= [|2,4\rangle + \tau|4,2\rangle + \zeta\,(|1,3\rangle + \tau|3,1\rangle)]/2,\\
|3,(\tau,\zeta)\rangle &= [|1,4\rangle + \tau|4,1\rangle + \zeta\,(|3,2\rangle + \tau|2,3\rangle)]/2.
\end{aligned} \tag{A.8}$$

In this basis the action of the t–J Hamiltonian results in a 3×3 matrix for the singlet ($\tau = 1$) sector:

$$\begin{pmatrix} -J & 0 & -(1+\zeta)t' \\ 0 & -J' & -(1+\zeta)t \\ -(1+\zeta)t' & -(1+\zeta)t & 0 \end{pmatrix}. \tag{A.9}$$

The ground state energy E in the singlet sector ($\tau = 1$ with $\zeta = 1$) is found from the solution of the third-order equation

$$-(J+E)(J'+E)E + 4(E+J)t^2 + 4(E+J')t'^2 = 0, \tag{A.10}$$

which can be easily solved in the symmetric case $t' = t$, $J' = J$:

$$E = -\tfrac{1}{2}\left(J + \sqrt{J^2 + 32t^2}\right). \tag{A.11}$$

In the asymmetric case (20*a*) with $\alpha = J/t \ll \alpha' = J'/t'$ one can derive an iterative solution treating the term

$$-(J'+E)E + 4t^2 = -4\frac{E+J'}{E+J}t'^2 \tag{A.12}$$

on the right-hand side of (A.12) as a perturbation. The resulting ground state energy in first order of this perturbation reads

$$E_0^{(\mathrm{p})} = E_a^{(\mathrm{p})} + \Delta E_a \tag{A.13}$$

$$\Delta E_a = -4\frac{E_a^{(\mathrm{p})} + J'}{E_a^{(\mathrm{p})} + J}\frac{t'^2}{\sqrt{J'^2 + 16t^2}} \tag{A.14}$$

where

$$E_a^{(\mathrm{p})} = -\tfrac{1}{2}\left(J' + \sqrt{J'^2 + 16t^2}\right). \tag{A.15}$$

For example, for $J = 0.5$, $J' = 4$, $t' = 1$ the correction term (A.14) yields a 3% contribution to the ground state energy E, such that the zeroth-order $E_a^{(\mathrm{p})}$ is already a very good approximation.

In the regime (20*b*) with $\alpha' = J'/t' \ll \alpha = J/t$ we derive from (A.10) a corresponding ground state energy in a first-order perturbation:

$$E_0^{(\mathrm{p})} = E_b^{(\mathrm{p})} + \Delta E_b \tag{A.16}$$

$$\Delta E_b = -4\frac{E_b^{(\mathrm{p})} + J}{E_b^{(\mathrm{p})} + J'}\frac{t^2}{\sqrt{J^2 + 16t'^2}} \tag{A.17}$$

where

$$E_b^{(\mathrm{p})} = -\tfrac{1}{2}\left(J + \sqrt{J^2 + 16t'^2}\right). \tag{A.18}$$

Let us now turn to the triplet sectors ($\tau = -1$). Here the six eigenstates and corresponding eigenvalues turn out to be

$$\begin{aligned}
&|1,(-1,-1)\rangle && E = 0\\
&|2,(-1,-1)\rangle && E = 0\\
&\frac{1}{\sqrt{2}}\left(|1,(-1,1)\rangle \mp |3,(-1,1)\rangle\right) && E = \pm 2t'\\
&\frac{1}{\sqrt{2}}\left(|2,(-1,1)\rangle \mp |3,(-1,-1)\rangle\right) && E = \pm 2t.
\end{aligned}$$

(d) $Q = 3$, $N_{\mathrm{c}}(3) = 12$

We introduce $|m,n\rangle$ as $Q = 3$ basis state with the hole (0) at plaquette position m and spin-down electron ($-$) at position n. The creation operators of the two spin-up electrons (+) and that of the spin-down electron ($-$) are ordered according to the increasing site number (cf figure A.1). For example, $|1,3\rangle \equiv c^+_{2\uparrow}c^+_{3\downarrow}c^+_{4\uparrow}|0\rangle$.

In the basis

$$\begin{aligned}
|1,\tau,\zeta\rangle &= [(|4,2\rangle + \tau|1,3\rangle) + \zeta(|3,1\rangle + \tau|2,4\rangle)]/2,\\
|2,\tau,\zeta\rangle &= [(|4,3\rangle + \tau|1,2\rangle) + \zeta(|3,4\rangle + \tau|2,1\rangle)]/2,\\
|3,\tau,\zeta\rangle &= [(|4,1\rangle + \tau|1,4\rangle) + \zeta(|3,2\rangle + \tau|2,3\rangle)]/2,
\end{aligned} \tag{A.19}$$

the t–J Hamiltonian reduces to the following 3×3 matrix for the eigenvalues with $x = J/2$, $x' = J'/2$:

$$\begin{pmatrix}
\zeta\tau t' - x & 0 & -\zeta t + x\\
0 & -\zeta t - x' & \zeta\tau t' + x'\\
-\zeta t + x & \zeta\tau t' + x' & -x - x'
\end{pmatrix}. \tag{A.20}$$

The eigenvalues are given by

$$E^{(\mathrm{p})}(\tau,\zeta) = -(x + x') \pm \sqrt{A^{(\tau)} + \zeta B^{(\tau)}}, \qquad \zeta(\tau t' - t), \tag{A.21}$$

with

$$\begin{aligned}
A^{(\tau)} &= (x^2 - xx' + x'^2) + (t^2 + \tau t t' + t'^2),\\
B^{(\tau)} &= -(2t + \tau t')x + (2\tau t' + t)x'.
\end{aligned} \tag{A.22}$$

The four eigenstates corresponding to the eigenvalues $\zeta(\tau t' - t)$ which are independent of the spin couplings J, J' have maximal total spin $S = 3/2$. The remaining ones have total spin $S = 1/2$.

For the choices (15a), (15b) of plaquette parameters (t, J, t', J') the ground state is given by one of the J, J'-dependent ($\tau = 1$) states with energy

$$E^{(\mathrm{p})}(\tau = 1,\zeta) = -\left(x + x' + \sqrt{A^{(1)} + \zeta B^{(1)}}\right). \tag{A.23}$$

The ground state in the symmetric case $t' = t$, $J' = J$,

$$E^{(\mathrm{p})}(\tau,\zeta = \pm 1) = -J - \sqrt{\left(\frac{J}{2}\right)^2 + 3}, \tag{A.24}$$

is twofold degenerate with respect to the quantum number $\zeta = \pm 1$. This degeneracy is lifted in the asymmetric case (A.23) if the term $B^{(1)}$ (A.22) is nonvanishing.

(e) $Q = 4$, $N_c(4) = 6$

We introduce $|m, n\rangle$ as the $Q = 4$ basis state with the two spin-up particles (+) at plaquette positions m and n. Again, we use the definition that all creation operators of the four electrons 2(+), 2(−) act in order of increasing site number (cf figure A.1) on the vacuum $|0\rangle$ (e.g. $|1, 3\rangle \equiv c^+_{1\uparrow}c^+_{2\downarrow}c^+_{3\uparrow}c^+_{4\downarrow}|0\rangle$).

In the basis

$$\begin{aligned} |1, \tau\rangle &= \frac{1}{\sqrt{2}}(|1, 3\rangle + \tau|2, 4\rangle) \\ |2, \tau\rangle &= \frac{1}{\sqrt{2}}(|1, 2\rangle + \tau|3, 4\rangle) \\ |3, \tau\rangle &= \frac{1}{\sqrt{2}}(|1, 4\rangle + \tau|2, 3\rangle) \end{aligned} \tag{A.25}$$

the t–J Hamiltonian reduces to the matrix

$$\begin{pmatrix} -J & 0 & \Delta\tau J \\ 0 & -J' & \Delta\tau J' \\ \Delta\tau J & \Delta\tau J' & -(J + J') \end{pmatrix}. \tag{A.26}$$

with $\Delta\tau = (1 + \tau)/2 = 1, 0$.

The eigenvalues for $\tau = -1$ are simply given by

$$E^{(p)}(Q = 4, -) = -J, -J', -(J + J'), \tag{A.27}$$

whereas the case $\tau = 1$ yields

$$E^{(p)}(Q = 4, +) = -(J + J') \pm \sqrt{J^2 + J'^2 - JJ'}, 0. \tag{A.28}$$

The ground state for all parameter values is uniquely given in the $\tau = 1$ sector.

Appendix B. First-order perturbation theory

To see the effects of first-order perturbation theory in the hopping parameter t'', we start from the transition matrix elements:

$$\begin{aligned} t'' &\left\langle \prod_{j=1}^{N/4} \psi_0^{(p)}(Q'_j) \left| \sum_{j=1}^{N/4} h_{j,j+1}(\alpha') \right| \prod_{j=1}^{N/4} \psi_0^{(p)}(Q_j) \right\rangle \\ &= t'' \sum_{j=1}^{N/4} A_{j,j+1} \left\langle \psi_0^{(p)}(Q'_j)\psi_0^{(p)}(Q'_{j+1}) \middle| h_{j,j+1}(\alpha') \middle| \psi_0^{(p)}(Q_j)\psi_0^{(p)}(Q_{j+1}) \right\rangle \end{aligned} \tag{B.1}$$

with

$$A_{j,j+1} = \prod_{l \neq j,j+1} \delta_{Q_l Q_l}. \tag{B.2}$$

The interaction Hamiltonian $h_{j,j+1}(\alpha')$ between neighbouring plaquettes is illustrated in figure B.1. The hopping part $h^{(t)}_{j,j+1}$ is active if the two links $\langle xx'\rangle\langle yy'\rangle$ are occupied by one electron and one hole, respectively. This means, in terms of occupation numbers $n(x), n(x')$ on the sites x, x', $n(x) = 1, n(x') = 0$ or $n(x) = 0, n(x') = 1$. Therefore, the hopping term induces a charge exchange by one unit

$$h^{(t)}_{j,j+1}: \quad (Q_j, Q_{j+1}) \to (Q_j - 1, Q_{j+1} + 1), \qquad (Q_j + 1, Q_{j+1} - 1) \tag{B.3}$$

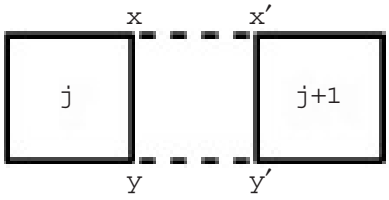

Figure B.1. Leg couplings (x, x'), (y, y') linking the neighbouring plaquettes j and $j+1$ on the ladder.

between neighbouring plaquettes. Note, in particular, that charge exchange by two and more units like in (54) is forbidden in first-order perturbation theory.

Therefore the nonvanishing matrix elements

$$\left\langle \psi_0^{(\mathrm{p})}(Q'_j)\psi_0^{(\mathrm{p})}(Q'_{j+1}) \middle| h_{j,j+1}(\alpha') \middle| \psi_0^{(\mathrm{p})}(Q_j)\psi_0^{(\mathrm{p})}(Q_{j+1}) \right\rangle = W(Q_j, Q_{j+1})\delta_{Q'_j,Q_j}\delta_{Q'_{j+1},Q_{j+1}} \quad \text{(B.4)}$$

are necessarily diagonal for the pairs of interest:

$$(Q_j, Q_{j+1}) = (0,2), (0,4), (2,4), (0,0), (2,2), (4,4). \quad \text{(B.5)}$$

They arise from the spin exchange part $h^{(J)}_{j,j+1}$ which is active if both sites x, x' (cf figure B.1) are occupied with one electron:

$$h^{(J)}_{j,j+1} = \left(2\mathbf{S}(x)\mathbf{S}(x') + \tfrac{1}{2}\right) n(x)n(x'). \quad \text{(B.6)}$$

Here $\mathbf{S}(x)$ and $\mathbf{S}(x')$ are spin operators at sites x and x' and we get for the interaction energies $W(Q_j, Q_{j+1})$ for plaquette pairs (B.5)

$$W(Q_j, Q_{j+1}) = -t''\alpha' \frac{Q_j Q_{j+1}}{32} \quad \text{(B.7)}$$

if Q_j and Q_{j+1} come from equation (B.5).

References

[1] Bednorz J G and Müller K A 1986 *Z. Phys.* B **64** 189
[2] Anderson P W 1987 *Science* **235** 1196
[3] Emery V J, Kivelson S A and Lin H Q 1990 *Phys. Rev. Lett.* **64** 475
[4] Dagotto E, Moreo A, Ortolani F, Poilblanc D and Riera J 1992 *Phys. Rev.* B **45** 10741
[5] Putikka W O, Luchini M U and Rice T M 1992 *Phys. Rev. Lett.* **68** 538
Putikka W O, Glenister R L, Singh R R P and Tsunetsugu H 1994 *Phys. Rev. Lett.* **73** 170
[6] Fehske H, Waas V, Röder H and Büttner H 1991 *Phys. Rev.* B **44** 8473
[7] Valenti R and Gros C 1992 *Phys. Rev. Lett.* **68** 2402
[8] Hellberg C S and Manousakis E 1995 *Phys. Rev.* B **52** 4639
Hellberg C S and Manousakis E 1997 *Phys. Rev. Lett.* **78** 4609
Hellberg C S and Manousakis E 2000 *Phys. Rev.* B **61** 11787
Hellberg C S and Manousakis E 1999 *Phys. Rev. Lett.* **83** 132
[9] Calandra M, Becca F and Sorella S 1998 *Phys. Rev. Lett.* **81** 5185
[10] Rommer S, White S R and Scalapino D J 2000 *Phys. Rev.* B **61** 13424
Poilblanc D, Scalapino D J and Capponi S 2003 *Phys. Rev. Lett.* **91** 137203
Scalapino D J, White S R and Affleck I 2001 *Phys. Rev.* B **64** 100506
[11] Martins G B, Gazza C and Dagotto E 1999 *Phys. Rev.* B **59** 13596
Brunner M, Capponi S, Assaad F F and Muramatsu A 2001 *Phys. Rev.* B **63** 180511
Chiappa O, Capponi S and Poilblanc D 2001 *Phys. Rev.* B **63** 115120
Jurecka C and Brenig W 2001 *Phys. Rev.* B **63** 94409
[12] Bose I and Gayen G 1994 *J. Phys.: Condens. Matter* **6** L405
Bose I and Gayen G 1999 *J. Phys.: Condens. Matter* **11** 6427

[13] Frahm H and Kundu A 1999 *J. Phys.: Condens. Matter* **11** L557
[14] Zaanen J, Sawatzky G A and Allen J W 1985 *Phys. Rev. Lett.* **55** 418
[15] Jorgensen J D, Dabrowski B, Pei S, Hinks D G, Soderholm L, Morosin B, Schirber J E, Venturini E L and Ginley D S 1988 *Phys. Rev.* B **38** 11337
[16] Riera J, Poilblanc D and Dagotto E 1999 *Eur. Phys. J.* B **7** 53
[17] Park K and Sachdev S 2001 *Phys. Rev.* B **64** 184510
[18] Siller T, Troyer M, Rice T M and White S R 2001 *Phys. Rev.* B **63** 195106
[19] Fledderjohann A, Langari A and Mütter K-H 2003 *Eur. Phys. J.* B **36** 193